Journal of Drug Delivery Science and Technology 84 (2023) 104411

Contents lists available at ScienceDirect

Journal of Drug Delivery Science and Technology

journal homepage: www.elsevier.com/locate/jddst

Formulation of chrysin loaded nanostructured lipid carriers using Box Behnken design, its characterization and antibacterial evaluation alone and in presence of probiotics co-loaded in gel

Shaik Rahana Parveen [a], Sheetu Wadhwa [a,**], Molakpogu Ravindra Babu [a], Sukriti Vishwas [a], Leander Corrie [a], Ankit Awasthi [a], Farhan R. Khan [b], Maha M. Al-Bazi [c,d], Nahed S. Alharthi [e], Faisal Alotaibi [f], Gaurav Gupta [g,h], Narendra Kumar Pandey [a], Bimlesh Kumar [a], Popat Kumbhar [i], John Disouza [i], Monica Gulati [a,j], Jayanthi Neelamraju [k], Ratna Sudha Madempudi [k], Kamal Dua [j,l,m], Sachin Kumar Singh [a,j,*]

[a] School of Pharmaceutical Sciences, Lovely Professional University, Phagwara, Punjab, 144411, India
[b] College of Applied Medical Sciences AlQuwayiyah, Shaqra University, Saudi Arabia
[c] Department of Biochemistry, Faculty of Science, King Abdulaziz University, Jeddah, Saudi Arabia
[d] Experimental Biochemistry Unit, King Fahd Medical Research Center, King Abdulaziz University, Jeddah, Saudi Arabia
[e] Department of Medical Laboratory Sciences, College of Applied Medical Sciences, Prince Sattam Bin Abdulaziz University, Al Kharj, 11942, Saudi Arabia
[f] Department of Pharmacy Practice, College of Pharmacy, Shaqra University, Al-dawadmi, 11961, Saudi Arabia
[g] School of Pharmacy, Suresh Gyan Vihar University, Mahal Road, Jagatpura, Jaipur, India
[h] Department of Pharmacology, Saveetha Dental College, Saveetha Institute of Medical and Technical Sciences, Saveetha University, Chennai, India
[i] Department of Pharmaceutics, Tatyasaheb Kore College of Pharmacy, Warananagar, Tal: Panhala, Dist: Kolhapur, Maharashtra, 416113, India
[j] Faculty of Health, Australian Research Centre in Complementary and Integrative Medicine, University of Technology Sydney, Ultimo, NSW, 2007, Australia
[k] Unique Biotech, Plot no 677, Road no 34, Jubilee Hills, Hyderabad, Telangana, 500033, India
[l] Discipline of Pharmacy, Graduate School of Health, University of Technology Sydney, Ultimo, NSW, 2007, Australia
[m] Uttaranchal Institute of Pharmaceutical Sciences, Uttaranchal University, Dehradun, India

ARTICLE INFO

Keywords:
Chrysin
Probiotic
Nanostructured lipid carriers
Antibacterial activity

ABSTRACT

The present study deciphers formulation, optimization and characterization of chrysin nanostructured lipid carriers with probiotics (PB) loaded gel (*Chrysin* (CS)- Nanostructured lipid carriers (NLCs) + PB loaded gel) for topical application. Hot homogenization-probe sonication method was used to formulate NLCs. Formulation parameters were optimized using Box Behnken Design. The optimized formulation was characterized for particle size (PS), zeta potential (ZP), % entrapment efficiency (%EE), % drug loading (%DL). The optimized values were found to be 199.99 mg, 33.92 mg, 700 mg and 376.86 mg of solid lipid, liquid lipid, surfactant and co-surfactant respectively. The PS, ZP, % EE and % DL of optimized CS-NLCs + PB loaded gel were found to be 66.45 ± 5.62 nm, −22 ± 5.21 mV, 97.25 ± 0.15 and 82.3 ± 0.104, respectively. Transmission electron microscopic images revealed that NLCs loaded with CS were spherical in shape. The *in vitro* diffusion studies revealed that 98 ± 0.06% of CS got released from CS-NLCs + PB loaded gel at the end of 48 h. For initial 8h, release of CS was about 6-fold higher in case of CS-NLCs + PB loaded gel than that of naive CS gel and thereafter the release got reduced, which indicated the sustained release of CS from NLCs. The zone of inhibition of CS-NLCs + PB loaded gel was 0.5-fold, 0.2-fold and 0.54-fold higher than naive PB gel alone, naïve CS gel alone and CS-PB gel combination, respectively. It indicated significantly higher antibacterial activity of CS–NLCs + PB loaded gel as that of any other treatment group.

* Corresponding author. School of Pharmaceutical Sciences, Lovely Professional University, Phagwara, Punjab, 144411, India.
** Corresponding author. School of Pharmaceutical Sciences, Lovely Professional University, Phagwara, Punjab, 144411, India.
E-mail addresses: sheetupharma@gmail.com (S. Wadhwa), singhsachin23@gmail.com, sachin.16030@lpu.co.in (S.K. Singh).

https://doi.org/10.1016/j.jddst.2023.104411
Received 11 January 2023; Received in revised form 21 March 2023; Accepted 3 April 2023
Available online 6 April 2023
1773-2247/

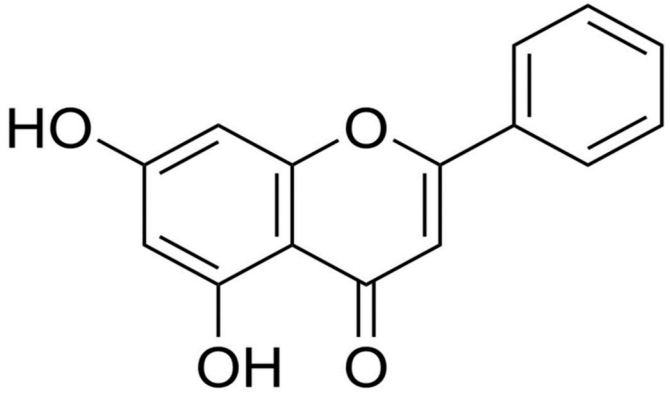

Fig. 1. Chemical structure of CS.

1. Introduction

Chrysin (CS) is chemically 5,7 di-hydroxy flavone with 15 carbons structure [1].The structure of CS is shown in Fig. 1. CS is abundantly present in natural sources like mushrooms (*Pleurotusostreatus),* propolis, blue passion flower (*Passifloracaerulaea)*, honey and baikal skullcap *(Radix scutellariae)*. CS has many potential pharmacological activities, which include neuroprotective, antienteroviral, anti-asthmatic, anti--depressant, antibacterial, anti-inflammatory, antiarthritic, anti-cancer, antiangiogenic, antimetastatic, immunomodulatory, and anti-proapoptotic effects [2,3]. Further, CS can also exert antipsoriatic effect by the regulation of mitogen activated protein kinase (MAPK), janaus kinase signal transducer and activator of transcription proteins signalling pathways (JAK-STAT), I- kappa B kinase/nuclear factor kappa light chain enhancer of activated B cells (IKK/NF-kB) signalling pathways. This leads to reduction of tumour necrosis factor-α (TNF-α), interleukin-17 A (IL-17 A), interleukin 22 (IL-22) induced chemokine (C–C motif) ligand 20 (CCL20) and antimicrobial peptides release from psoriatic skin epidermis. In addition, CS inhibits reactive oxygen species (ROS) production [4]. Considerably less number of oral formulations are reported for CS as it has limited by poor aqueous solubility and pre systemic metabolism [5]. Hence, a conventional topical route of administration can be considered (CTD) as an alternative to oral route of administration to deliver CS for the treatment of skin disease like psoriasis. However, CTD possess the challenges like poor penetration, less drug retention [6]. Hence, development of novel topical drug delivery is the most suggested system which can enhance the penetration and retention of drug through stratum corneum of skin. Thus, the CS loaded NLCs can improve the challenges faced by the CTD. NLCs are considered as the smarter, latest generation lipid nanoparticles, due to the presence of high drug loading capacity and entrapment efficiency [7,8]. In addition, the NLCs are highly stable due to the presence of preventive nature of the drug expulsion during storage.

It is pertinent to add that there is an important role of skin microbiome in maintaining the integrity of skin [9]. Some of the microbiome include *Firmicutes, Actinobcteria, Bacteroidetes and Proteobacteria* phyla, which maintains the skin homeostasis by acts like antimicrobial agent, forms physical barrier, regulates the immune system and kills the

Table 1
The design level and independent factors.

Factor	Levels		
	−1	0	+1
A: solid lipid (mg)	50	125	200
B: liquid lipid (mg)	25	62.5	100
C: surfactant (mg)	400	550	700
D: Co surfactants (mg)	225	337.5	445

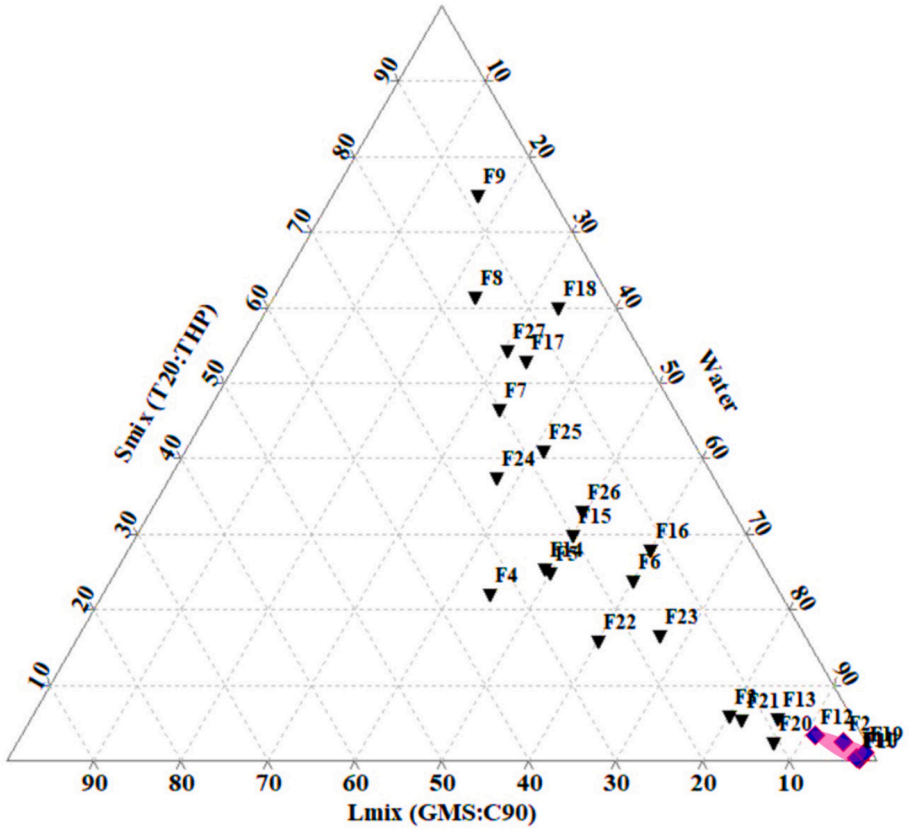

Fig. 2. Ternary phase diagram for initial screening of lipid composition.

Table 2
Study design protocol of zone of inhibition.

Group no.	Groups	Treatment	Dosage	No. of petri-plates
I	Normal control	Normal saline (no induction)	Spreaded on the solidified agar media	3
***Staphylococcus aureus* spread on the solidified agar petri-plates**				
II	Experimental control	*Staphylococcus aureus* (Test organism)	50 billion CFU spreaded on the solidified agar media	3
III	Positive control	Marketed Betamethasone cream	0.1% w/w filled in the 3 bores in each petri-plate	3
IV	Treatment I	Blank NLCs gel	Filled in the 3 bores in each petri-plate	3
V	Treatment II	CS gel	0.006% w/w of CS suspension filled in the 3 bores in each petri-plate	3
VI	Treatment III	CS NLCs gel	0.006% w/v of CS NLCs filled in the 3 bores in each petri-plate	3
VII	Treatment IV	PB gel	10 billion CFU BI UBBI-01 filled in the 3 bores in each petri-plate	3
VIII	Treatment V	CS(L) + PB gel	0.003% w/v of CS + 10 billions CFU BI UBBI-01 loaded filled in the 3 bores in each petri-plate	3
IX	Treatment VI	CS (H)+ PB gel	0.003% w/v of CS + 10 billions CFU BI UBBI-01 loaded filled in the 3 bores in each petri-plate	3
X	Treatment VII	Optimized CS NLCs (L) + PB loaded gel	0.0025% w/v of CS + 10 billions CFU BI UBBI-01 loaded NLCs filled in the 3 bores in each petri-plate	3
XI	Treatment VIII	Optimized CS NLCs $(H)_H$ + PB loaded NLCs gel	0.005% w/v of CS + 10 billions CFU BI UBBI-01 loaded filled in the 3 bores in each petri-plate	3

Note: L = Low dose; H= High dose; number of replicates (n) = 3.

pathogens [10,11]. It has been reported that skin injury, lack of microbiota of skin along with increased count of *Staphylococcus aureus*, decreased levels of *Actino bacteria, Macrococcus, Propionobacterium-granulosam*, *Staphylococcus epidermidis*, and *Propioni bacterium* are mainly responsible for skin disorders like psoriasis [12,13].

Considering the aforementioned skin dysbiosis probiotics like *Lactobacillus sakeiprobio 65(SEL001), Bifidobacterium infantis* UBBI-01 (BI) (BI) are considered as suitable therapeutic agents in the management of skin disorder like psoriasis by reduction of inflammatory mediators. Probiotics (PB) acts by producing the organic acids and reduce the pH of the skin [14,15]. In one of the clinical studies, it has been reported that BI upon oral administration reduced the levels of TNF-α, IL-6 and c-reactive protein (c-RP) [16]. Furthermore, BI also has been reported to maintain the "eubiosis" of skin upon topical administration [17].

Looking at the potential activity of probiotics, it has been decided to co-administer topically the probiotics along with the nano delivery system such as NLCs containing CS. In order to achieve this objective, the CS loaded NLCs (CS-NLCs) were prepared and the CS NLCs as well as probiotics were added in the gel. The NLCs will offer better penetration and drug retention at the topical site and CS as well as PB will elicit the pharmacological action at the site of application. The gel can be applied topically to get the triple benefits of NLCs, CS and PB. Preparation of NLCs by using formulation design requires sound scientific information about quality attributes and process variables. Optimization by one factor at a time (OFT) approach consumes more time and economically inefficient [18]. Factorial design is widely used for optimization by several researchers to overcome these challenges, which gives in depth relationship between dependent and independent variables [19]. Hence, in the present study an attempt was made to formulate the NLCs co loaded with CS-PB using Box Behnken design. (BBD). For that we have used 3 levels +1, 0, −1 and 4 factors i.e., solid lipid, liquid lipid, surfactant and co-surfactant. The CS-PB NLCs were formulated by modified hot homogenization followed by probe sonication technique and were investigated for particle size (PS), poly dispersity index (PDI), zeta potential (ZP), percentage entrapment efficiency (% EE), drug loading (% DL), *in vitro* drug release and antibacterial activity. The hypothesis as well as novelty lies in the unique nano-composition in the form of a topical delivery system, wherein, the CS is loaded in the NLCs for its better skin penetration and PB is suspended along with CS-NLCs in order to provide its anti-inflammatory effects. These CS-NLCs and PB are loaded in the gel for longer drug release and therapeutic benefits. Such formulation is being reported for the first time.

2. Materials and methods

CS was procured from the BLD Pharma tech Pvt. Ltd India (>98.0% purity), *Bifidobacterium infantis* UBBI-01 (BI) was a gift sample from Unique Biotech, Hyderabad, India. Glyceryl monosterate (GMS), Oleic acid (OA), Migolyol 812 (M 812), Isopropyl myristate (IPM) and Tween 80 (T80) were gift samples from Mohini organics Pvt. Ltd., India. Stearic acid (SA), palmitic acid (PA), Compritol® 888 pellets (CP-888), Emulcire 61^{TM}WL 2659 pellets (EM-P2659), Gelucire® 44/14(GS-44/14), Gelucire® 43/01 pellets (GSP-43/01), geleol (GL), capryol 90 (C-90), labrafil M 1944CS (LM1944CS), transcutol HP (T-HP), lauroglycol FCC (L-FCC), labrafaclabrafil WL1349 (LB-WL1349), and labrasol (LS) were gift samples from Gattefosse India. Capmul MCM (CMCM), Acconon MC8-2EP/NF (A-2EP/NF), poloxamer 188 (P-188) and poloxamer 407 (P-407) were obtained as gift samples from IMCD Pvt. Ltd, India. Paraffin oil (PO), Soyabean oil (S–O) and Tween 20 (T-20) were purchased from LobaChemie India. Nutrient agar was purchased from Himedia and *Staphylococcus aureus* procured from IMTECH Chandigarh.

Table 3
Characterization of selected CS loaded NLCs as per TPD.

Batch	Solid lipid	Liquid lipid	Surfactant	Co -surfactant	Ratios	PS (nm)	ZP (mV)	PDI	EE %	DL %
	GMS (mg)	C-90 (mg)	T-20 (mg)	T-HP (mg)						
F1	50	50	450	450	1:1	167 ± 64.99	−12.7 ± 10.22	0.101 ± 64.99	98 ± 1.26	8.7 ± 0.15
F2	100	100	400	400	1:1	133 ± 23.00	−16.5 ± 15.22	0.293 ± 23.00	98 ± 1.55	9.0 ± 0.89
F10	66	33	600	300	2:1	77 ± 13.88	−15.0 ± 10.22	0.271 ± 13.88	96 ± 0.66	9.0 ± 0.82
F11	133	66	533	266	2:1	147 ± 10.22	−15.5 ± 7.66	0.294 ± 10.22	90 ± 1.55	9.4 ± 0.78
F12	200	100	466	233	2:1	102 ± 11.25	−12.7 ± 8.99	0.294 ± 11.25	80 ± 0.89	9.0 ± 0.77
F19	75	25	675	225	3:1	82 ± 8.99	−15.6 ± 8.09	0.217 ± 8.99	98 ± 0.78	9.4 ± 0.77

Table 4
Screening of lipids as per TPD.

Batch	Lmix GMS:C-90 mg	Smix(T- 20:T-HP) mg									Water end point value (mL)
		9	8	7	6	5	4	3	2	1	
		1:1	1:1	1:1	1:1	1:1	1:1	1:1	1:1	1:1	
F1	50:50	450:450									100
F2	100:100		400:400								100
F3	150:150			350:350							4
F4	200:200				300:300						0.8
F5	250:250					250:250					1
F6	300:300						200:200				1.5
F7	350:350							150:150			0.5
F8	400:400								100:100		0.3
F9	450:450									50:5 0	0.2
		2:1	2:1	2:1	2:1	2:1	2:1	2:1	2:1	2:1	
F10	66:33	600:300									94
F11	133:66		533:266								72
F12	200:100			466:233							60
F13	266:133				400:200						1
F14	353:166					353:166					1
F15	400:200						266:133				1
F16	466:233							200:100			1.5
F17	533:266								133:66		0.5
F18	600:300									66:33	0.5
		3:1	3:1	3:1	3:1	3:1	3:1	3:1	3:1	3:1	
F19	75:25	675:225									100
F20	150:50		600:200								100
F21	225:75			525:175							4.5
F22	300:100				450:150						1.5
F23	375:125					375:125					2
F24	450:150						300:100				0.6
F25	525:175							225:75			0.7
F26	600:200								150:50		1.2
F27	675:225									75:25	0.5

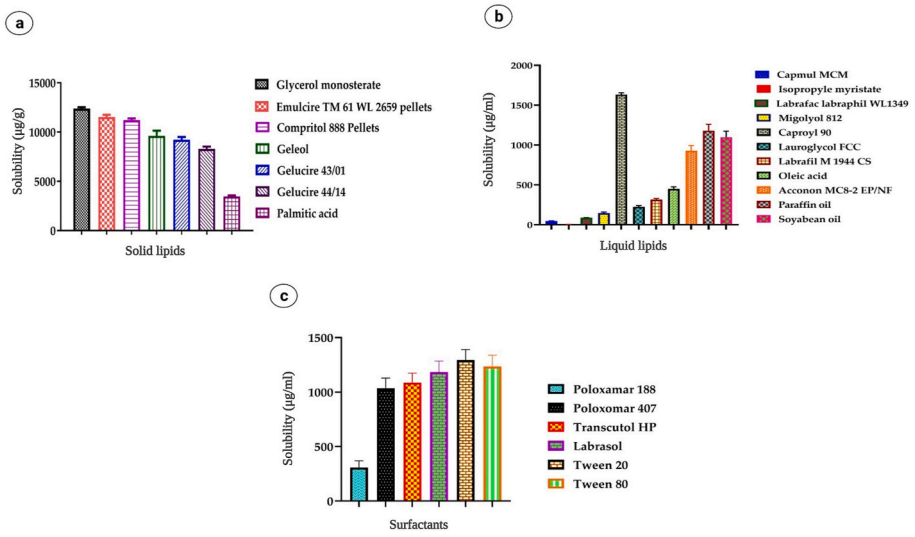

Fig. 3. Solubility of solid lipids (a), liquid lipids (b) and surfactant (c).

2.1. Experimental

2.1.1. Solubility study

Solubility studies were carried for solid lipids, liquid lipids and surfactants. Initially 1 g of each solid lipid (SA, PA, CP-888, GMS, GS-44/14, GL, GSP-43/01, EM-P2659) was taken in a beaker and it was placed on a magnetic stirrer at 100 °C [20,21]. The placed solid lipids were melted at 10 °C above their melting point and poured in a glass vial having 5 mL capacity [22]. A known excess amount of CS (50 mg) was added in it.Similarly, 1 mL of individual liquid lipids (CAP-MCM, IPM, LBWL1349, M812, PO, C-90, LM-1944CS, OA,S–O, L-FCC) and 1 mL of surfactants (T-HP, LB-WL1349, LS, T-20,L-FCC, LB-WL1349, CMCM, A-2EP/NF, P-188, P-407) were added individually in separate glass vials. Then all the lipids and surfactant mixtures were vortexed for 10 min [23]. Later all the glass vials were stoppered and kept in shaker water bath for 72 h at 37 ± 0.2 °C. Then all the samples were centrifuged at 10000 *g* for 10 min to separate the dissolved CS from saturated solution except solid lipids. A supernatant was collected and it was dissolved in methanol followed by filtration through 0.4 μm membrane filter [24]. The drug concentration was determined from the resultant samples by HPLC chromatography (Shimadzu LC-20AD Prominence) with a photodiode array detector (SPD-M20A Prominence Diode Array

Table 5
The data of responses for all the experimental runs designed by BBD for CS loaded NLCs.

Formulations	Independent variables				Responses		
	GMS (mg)	C-90 (mg)	T20 (mg)	THP (mg)	PS (nm)	ZP (mV)	% EE
F1	125	62.5	400	450.0	133	−16.8	96
F2	125	62.5	550	337.5	169	−19.9	95
F3	200	62.5	550	225	136	−19.25	94
F4	50	62.5	550	450	199	−18.9	93
F5	200	62.5	700	337.5	98.6	−20.3	96
F6	125	62.5	400	225	91	−21.2	92
F7	200	62.5	400	337.5	58	−18.6	98
F8	125	25	550	225	151	−19.48	95
F9	200	62.5	550	450	100	−16.7	93
F10	50	100	550	337.5	198	−20.1	89
F11	50	25	550	337.5	140	−18.06	97
F12	50	62.5	400	337.5	173	−18.7	97
F13	125	62.5	550	337.5	169	−19.9	94
F14	125	100	700	337.5	110	−22.3	89
F15	125	62.5	550	337.5	169	−19.9	96
F16	50	62.5	700	337.5	137	−19.88	96
F17	125	100	550	450	169.6	−19.6	88
F18	50	62.5	550	225	186.8	−17.6	93
F19	200	25	550	337.5	91.91	−19.9	95
F20	125	62.5	700	450	87.25	−21.4	86
F21	125	62.5	700	225	151	−18.6	95
F22	125	25	400	337.5	74	−20.3	94
F23	125	100	400	337.5	100	−19.7	96
F24	125	62.5	550	337.5	172	−19.9	95
F25	125	100	550	225	117.1	−20.6	85
F26	125	25	700	337.5	73.66	−20.3	96
F27	125	62.5	550	550	169	−19.00	94
F28	125	25	550	550	79	−19.54	89
F29	200	100	550	550	90	−19.32	96

Table 6
Summary of ANOVA results for all responses.

Response	Sequential p-value	Adjusted R^2	Predicted R^2	Suggested model	Sequential model sum of squares P-Value
Particle size	<0.0001	0.9886	0.9967	Quadratic	<0.0001
ZP	<0.0001	0.9376	0.8841	Quadratic	<0.0001
% EE	<0.0001	0.9064	0.7667	Quadratic	<0.0001

Detector), Rheodyne injector (7725i) of 20 μL loop and C-18 column (Nucleodur C_{18}, 250 mm × 4.6 mm i.d.,5μ, 100 ^{0}A in isocratic mode of elusion. The mixture of methanol and 0.1% v/v formic acid in 70:30 v/v ratio was used as mobile phase. A standard calibration curve was plotted by taking known concentrations of CS from 2 to 10 μg/mL. The curve was found linear with r^2 value of 0.9987. The amount of CS dissolved in each excipient was measured at 268 nm [25].

2.1.2. Construction of pseudo ternary phase diagram

2.1.2.1. Initial screening of formulation development. To identify the existence of the nanoemulsion region pseudo ternary phase diagram was constructed using aqueous titration method. Based on the results of solubility studies GMS was selected as solid lipid, C-90 as liquid lipid, T20 as surfactant and T-HP as co surfactant. The ratio of components was determined by the aqueous titration method corresponding to the region of nanoemulsion. Initially, the mixture of lipids (Lmix) and surfactants (Smix) were taken in the ratios of 1:1, 2:1 and 3:1 (External ratios). Further, within the selected two lipids and two surfactants, various ratios (internal ratios) were taken, which resulted in nine prototype formulations in each external ratio [26]. So, a total of 27 formulations (F1–F27) were prepared and observed visually. A ternary phase diagram (TPD) was drawn using ternary software (Triplot software version 4.1.2) to identify the existence of nanoemulsion region. Among 27 formulations only 6 formulations (F1, F2, F10, F11, F12 and F19) were transparent and clear which are converted into NLCs. These represented by various colored regions in the TPD. Further, they were analyzed for PS, PDI, ZP, %EE and % DL. The remaining formulation shown opaque and phase separation nature which were depicted in Fig. 2.

2.1.3. Optimization of CSloaded NLCs by BBD

2.1.3.1. Design of experiment (DoE). The NLCs were optimized by using BBD (DOE stat/Ease USA version 11.1.2.0.lic) on the basis of results of initial screening. Based on the results TPD four independent variables i.e., amount of GMS (solid lipid), C-90 (liquid lipid), T-20 (surfactant) and Transcutol HP (Co surfactant) were taken. Each factor was tested at three levels, which were designated as −1, 0 and + 1. Three responses were recorded for the study which includes PS, ZP and % EE. A total 29 runs (formulations) were designed by the software. The amount of drug (CS) kept constant in all 29 formulations [27]. To increase the predictability of the model all the experiments were run in random order. The design level and independent factor are shown in Table 1.

2.1.4. Preparation of CS NLCs

The CS NLCs were prepared by using modified hot homogenization technique followed by probe sonication. The quantities of GMS, C-90, T-20 and T-HP were taken as per the quantities given by DoE which was shown in Table 2. Initially CS was dissolved in C-90 (liquid lipid). Simultaneously solid lipid (GMS) was melted in a beaker above its melting point (80 °C). The mixture of CS with C-90 was added to the molten GMS during heating, which was considered as lipid phase. On the other hand, T-20 as well as T-HP were added to 9 mL of double distilled water and heated at the same temperature, which was considered as aqueous phase. The lipid phase (mixture of solid lipid, liquid lipid along with drug) was added to aqueous phase (surfactants and co surfactants mixture) and subjected to homogenization at 4000 rpm for 45 min. After that, mixture is placed in sonicator for 15 min followed by probe sonication for 5 min to reduce the particle size and to improve the PDI [28].

2.1.5. Preparation of CS NLCs and PB loaded gel

To prepare CS NLCs and PB loaded gel, initially carbopol 940 (1%w/w) was employed as a gelling agent. In order to achieve a homogenous dispersion, 2 g of carbopol 940 was dissolved in 200 mL of CS NLCs while being stirred on a magnetic agitator at 1500 rpm. The pH was adjusted to 6.8 by adding triethanolamine before the mixture was neutralized. Finally, 0.2 g of *Bifidobacterium infantis* UBBI-01 (BI) (contains 10 billion CFU was added as PB to this dispersion to produce the CS NLCs and PB loaded gel.

2.1.6. Characterization of CS NLCs, CS-NLCs and PB loaded gel

2.1.6.1. Particle size (PS), poly dispersity index (PDI) and zeta potential (ZP). The PS, ZP and PDI of the developed CS-NLCs and CS-NLCs PB loaded gel were evaluated by zeta sizer (Nano ZS90, Malvern Instruments Ltd., India) fitted with a 532 nm laser at a fixed scattering angle of 173°. The sample analysis was carried out by passing a dynamic light scattering via sample filled disposable cuvette at 25 °C temperature. The sample was diluted up to 10 times with double distilled water and were filtered through a 5 μm cellulose membrane before performing the analysis [29]. In similar manner, ZP also analyzed by placing same sample in electrode containing cuvette [28]. Each sample was recorded in triplicate with standard deviation.

2.1.6.2. % Entrapment efficiency (%EE) and % drug loading (%DL). The

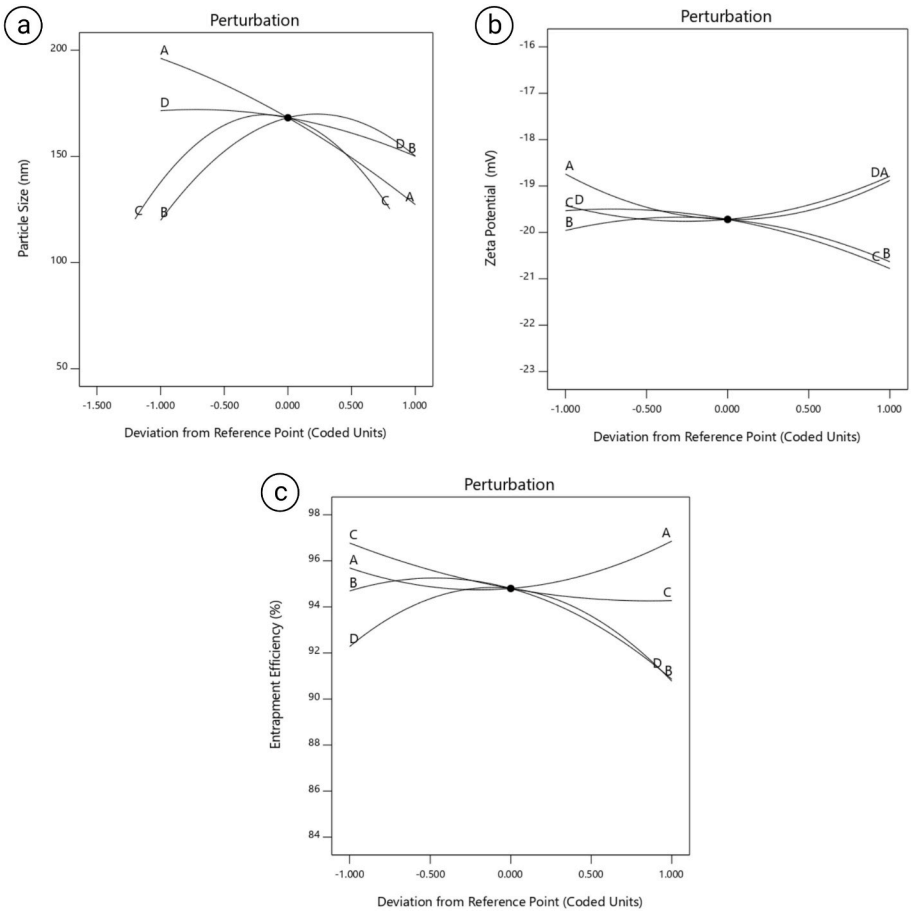

Fig. 4. (a–c). Perturbation plots indicating the impact of factors A, B, C and D on responsesa.PS, b. ZP and c. % EE.

CS loaded NLC sample was tested for drug loading and entrapment efficiency percentage determination. Firstly, the amount of CS (initial amount of total CS) was determined by UV–visible spectrophotometer by diluting the NLCs dispersion with methanol up to 200v folds [30]. Consequently, the % DL and % EE of CS was determined by centrifugation method. An aliquot of 2 mL of NLCs dispersion was taken in Eppendorf and centrifuged (Remi Elektrotechnik Ltd-India) at 10000 rpm for 15 min to separate the unloaded CS. The supernatant was then diluted with methanol, filtered through membrane filter (0.2 μm cut off) and analyzed by HPLC method mentioned section 2.1.1 at 268 nm. The % EE of CS was calculated by equation 1 [31,32].

$$\%\ EE = \frac{\text{Amount of initial drug} - \text{Amount of free drug}}{\text{Amount of initial drug}} \text{X } 100 \qquad \text{equation (1)}$$

The amount of CS loaded in the lipids was determined by using equation (2)

$$\%DL = \frac{\text{Weight of initial drug} - \text{weight of free drug}}{\text{weight of total lipid}} \times 100 \qquad \text{equation (2)}$$

2.1.6.3. High resolution transmission electron microscopy (HRTEM) of CS-NLCs. The internal morphology of optimized formulation was determined by using HR-TEM (JEM -2100 PLUS electron microscope, Jeol, India). The scanning was done at 200 KV with 15 lakhs maximum magnification and 0.194 nm resolution. A drop of formulation was diluted with water and negative staining was done using 2% w/v of phosphotungstic acid. The excess liquid present on the film was wiped out by a filter paper and the grid was dried of at room temperature [33].

2.1.7. Determination of zone of inhibition of developed formulation

2.1.7.1. Antibacterial study. The zone of inhibition of the optimized formulation was determined by antibacterial studies at lower and higher doses. The study was designed with 8 treatment groups along with normal, experimental and positive control. The study design is shown in Table 3. The study was done in triplicate using 3 petri-plates for each group. Each petri-plate was containing 15 mL of sterilized agar medium. The plates were kept in an aseptic laminar air flow environment to maintain sterile condition. These petri plates were kept aside for 30–45 min for solidification. After that, 3 bores were made in each petri plate followed by the addition of inoculums of *Staphylococcus aureus* except normal control. The specified dosing as mentioned in Table 3 was filled into the bores of petri-plates and plates were incubated in an incubator for 48 h at 37 °C [34].

2.1.8. In vitro diffusion study

The diffusion profiles of naïve CS gel, CS-NLCs, CS NLCs and PB loaded gel, were carried out by Franz diffusion cell (FDC) with the help of dialysis membrane. The molecular cut off of the membrane was 12 KD. The membrane was soaked in 100 mL phosphate buffer (PBS) of pH6.8 for 24 h for activation before its use. The receiver compartment of FDC was filled with 17 mL of phosphate saline and methanol in 7:3 v/v ratio. The previously soaked membrane was kept in between donor and receptor compartment. The donor compartment was filled with 1 g of CS NLCs and PB loaded gel, and the total assembly was kept on magnetic stirrer at 150 rpm. The temperature was maintained at 37 °C using thermostatically controlled magnetic stirrer. At fixed intervals of time (0.5, 1, 2, 4, 6, 12, 24, 32, 36, 40, 44 and 48 h) samples were withdrawn (1 mL) and sink condition was maintained. The samples were analyzed

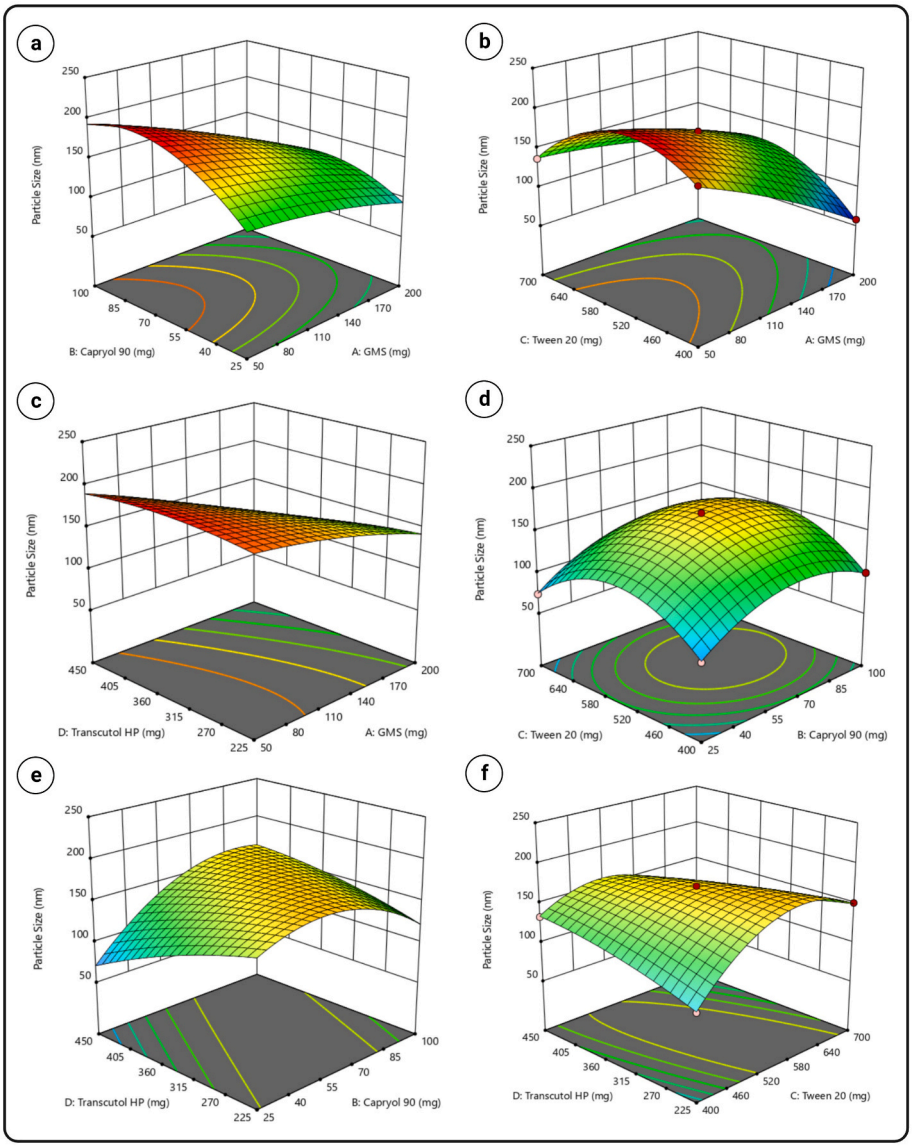

Fg. 5. (a–f). 3DRSP showing the effect of factor A, B, C and D on PS.

by HPLC to determine the amount of drug diffused. Similar experiments were carried out with naïve CS gel CS NLCs. All the results are recorded in triplicate manner [35]. The release pattern of CS-NLCs and CS-PB NLCs was evaluated by applying various mathematical models like Zero order, First order, Higuchi, Hixson–Crowel and Krosmeyer- Peppas equations.

2.1.9. Stability studies

The optimized CS-NLCs and PB loaded gel was subjected to stability studies as per ICH Q1(R2) and conducted at two storage conditions i.e., 25 ± 0.2 °C with 65% ± 5% RH and 5 ± 0.2 °C for 6 months. The samples were withdrawn at the end of 3rd and 6th month. They were further evaluated for PS, PDI, ZP, and %EE . Their results were compared with the results of fresh formulation. All the results were recorded in triplicate [35,36].

3. Results and discussion

3.1. Solubility studies

The selection of solid lipids, liquid lipids, surfactants and co-surfactants for the development of CS loaded NLCs was done on the basis of a solubility studies. Among the selected six solid lipids, the solubility of CS was found in the following descending order:GMS (12376 ± 4.582 μg/g) >EM-P2659(11513 ± 2.213 μg/g) >CP888 Pellets (11191 ± 1.1191 μg/g) > GL (9620 ± 14.422 μg/g) >Gelucire 43/01 (9210 ± 8.6602 μg/g) > Palmitic acid (3456 ± 2.0816 μg/g). It has been observed that CS showed highest solubility in GMS, which may be attributed the presence of the lower HLB (3.8) [37] and nearer to the log P value of CS (3.2) [38]. It has been reported that the CS NLCs prepared by using GMS as solid lipid shown higher % EE and sustained release [39,40]. Several reported research studies used GMS as solid lipid for the development of NLCs For instance Koland and Sindhoor (2021) prepared GMS based NLCs for psoriasis treatment and the results shown higher permeability and retetion of apremilast upon topical administration [41]. Another research performed by Pimpalshende et al. (2018) revealed that stable NLCs were formulated when GMS was used as solid lipid for formulation of betamethasone dipropriate NLCs for topical application [42]. NLCs prepared by the GMS as solid lipid have been reported to produce the smaller PS in the range of 57–179 nm and showed better release of drug [43].

Among the selected nine liquid lipids, the solubility of CS was found

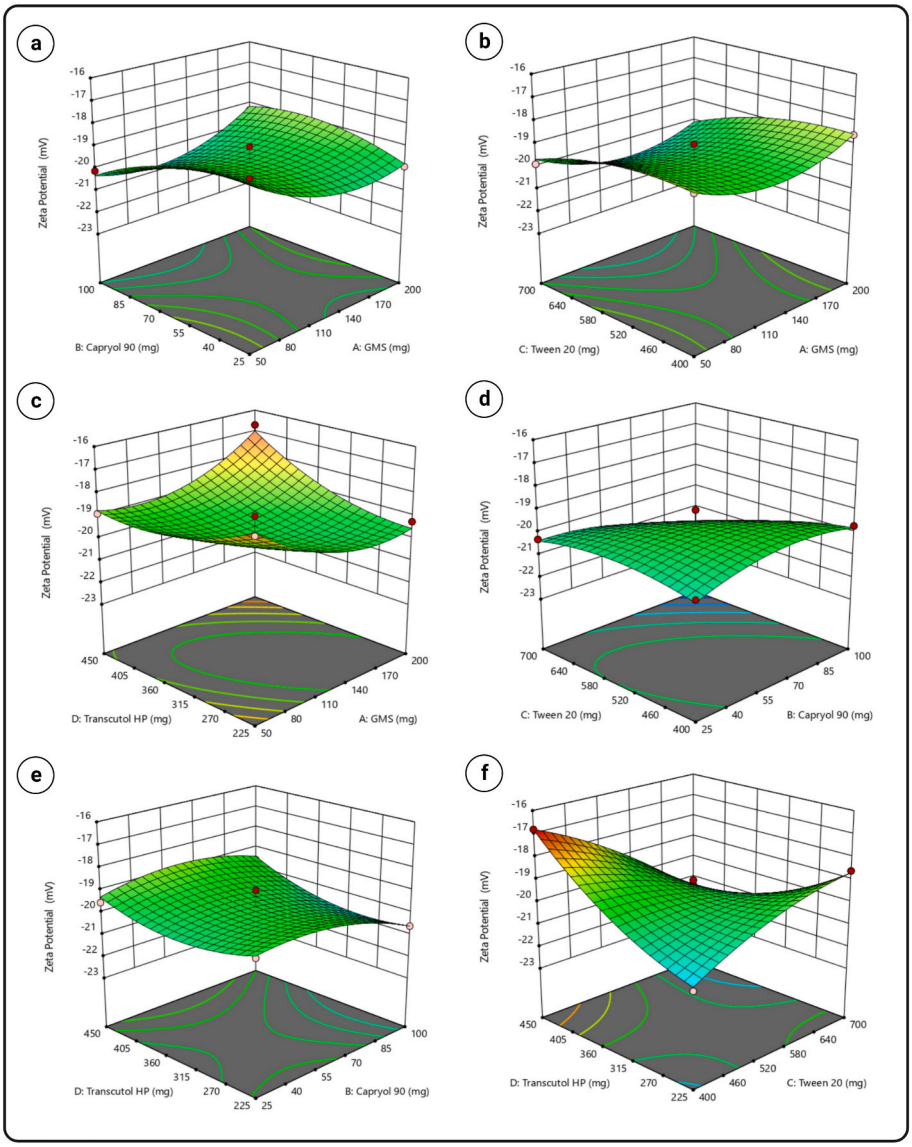

Fig. 6. (a–f). 3D RSP showing the effect of factor A, B, C and D on ZP.

in the following decreasing order in μg/mL: Capryol 90 (1179 ± 1.155 μg/mL) >Soyabean oil (1098 ± 15.716 μg/mL) >Acconon MC8 (928. 667 + 4.509 μg/mL) > Oleic acid (450.667 ± 5.033 μg/mL) >Lauroglycol FCC (224.33 ± 5.686 μg/mL) > Paraffin oil (163.53 ± 2.040 μg/mL) >Migolyol 812 (147.43 ± 2.205 μg/mL) > Labrafac Labraphil WL1349 (86.20 ± 2.030 μg/mL) > Capmul MCM (46. 667 ± 2.309 μg/mL).

C90 was selected as liquid lipid due to the presence of higher solubility of CS in it. it has been reported that incorporation of liquid lipid into solid lipid improves the %EE and DL due to the development of imperfections in the solid lipid [43]. Further more liquid lipid may reduce the crystalline nature of solid lipid that could help in improving the physical stability of dispersion system. It was confirmed by one of the previous study, reported by Guy et al., in 2019, whereas C-90 was used as liquid lipid for development of NLCs loaded with triptolide for the treatment of rheumatoid arthritis [44]. In addition to that C90 was also able to induce the surface charge on particles. It was very essential for getting the stable dispersion system. Abdel-Salam et al. in 2017 incorporated the C-90 as liquid lipid for development of diflucortolone valerate NLCs for topical administration which shown higher permeability [45].

Among selected six surfactants, CS has shown highest solubility in T-20 in the following decreasing order in μg/mL: T-20 (1295 ± 4.747) > T-80 (1236 ± 53.44) > LB (1184 ± 0.577) > T-HP (1087 ± 16.92) > P-407 (1037 ± 2.532) > P188 (308 ± 1.155).

The T-20 has been reported to reduce the interfacial tension between water and lipids efficiently, and imparts viscosity for maintaining the stability of the dispersion system. For example, V. M Ghate et al. (2019) employed the T-20 as surfactant for development of pentoxifylline NLCs for psoriasis. In addition to that T-20 also provides shielding effect around the particles [46].

Further, T-HP was selected as co surfactant to improve the permeability of the CS across the skin. In addition, T-HP was able to enhance the solubilization and emulsification of surfactant by raising the interfacial fluidity of surfactants as an external surface in the micelles. Further, T-HP readily permeates through the stratum corneum and by the interaction of the water present in the intercellular path, it will modify the skin permeation of the active drug [47]. Makky*et al.*, in 2021 used the T- HP as co-surfactant for the development of caffeine loaded NLCs for treating alopecia [48].

From the results of solubilization studies GMS as solid lipid, C-90 as liquid lipid, T-20 as surfactant and T-HP as cosurfactant have been

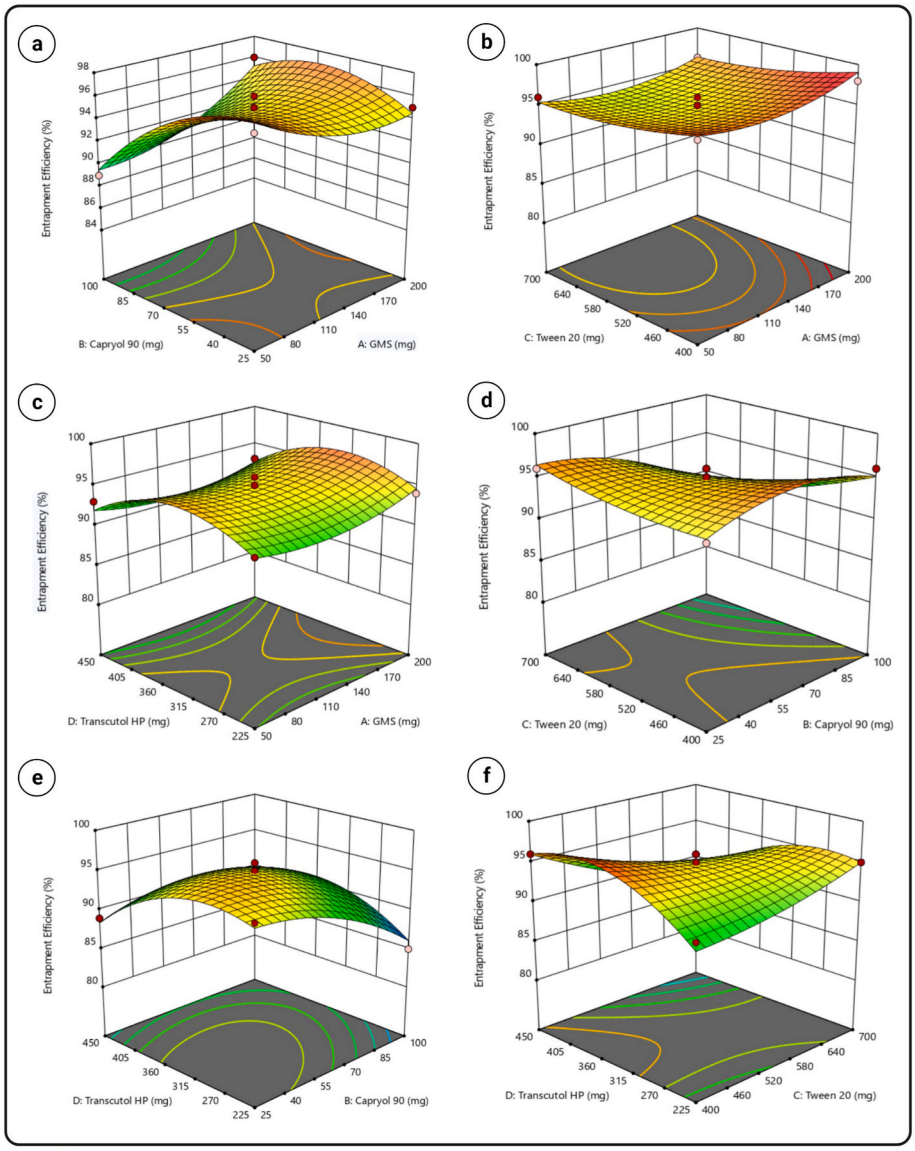

Fig. 7. (a–f). 3D RSP showing the effect of factor A, B, C and D on % EE.

selected. By considering the results of previously reported individual studies, the combination of GMS, C-90, T-20 and T-HP could be able to offer good formulation characteristics. The results of solubility studies have been depicted in (Fig. 3a, Fig. 3b and c) showing the highest solubility of CS in solid lipid, liquid lipid, surfactant and cosurfactant.

3.2. TPD

On the basis of the TPD, a total of 27 formulations were prepared in the ratio of 1:1, 2:1 and 3:1 of Lmix and Smix as shown in Table 4. The transparent formulations were considered for further study and they were considered as nanoemulsion. According to TPD formulations F1, F2, F10, F11, F12 and F19 were observed as transparent and evaluated further for PS, ZP, PDI,%EE and %DL [49]. The results of (Table 5) PS and ZP of all six, CS loaded nanoemulsion showed less than 200 nm and PDI less than 0.3, which indicated the formulation are in nano size and are well dispersed respectively. ZP was found in the range of −12.7 mV to −16.5 mV, which indicated the presence of the repulsive forces between the particles and nanoemulsion were stable. It may be due to the non-ionic property of surfactant. The % EE was found between the 87–94% which indicated the better entrapment efficiency of lipids for CS and optimum loading. Hence three levels (low, medium, high) of solid lipid, liquid lipid, surfactant and co-surfactant were taken for further study by DoE.

3.3. BBD

A total of 29 experiments were carried out with BBD to study the effect of excipients used to formulate NLCs (solid lipid, liquid lipid, surfactant and co-surfactant) on PS, ZP and EE. The data of responses for all the experiments runs designed by BBD is depicted in Table 2. The magnitude and significance of the effects of main variables and their interactions were determined by analysis of variance (ANOVA). The counter plots for independent factors were generated by the use of the obtained polynomial equations (PE) from BBD. The adequacy of the model was confirmed by the use of ANOVA i.e., ($P < 0.05$). The summary of results for all responses was shown in Table 6. The results of ANOVA for all responses are shown in Table 6. The polynomial equations explained that solid lipid, liquid lipid, surfactant and co-surfactant have significant effects on PS, ZP, and % EE. All the equations (eq. (3), eq. (4) and eq. (5)) for PS, ZP and % EE respectively were quadratic. The coded factors determined by design expert software are shown in below

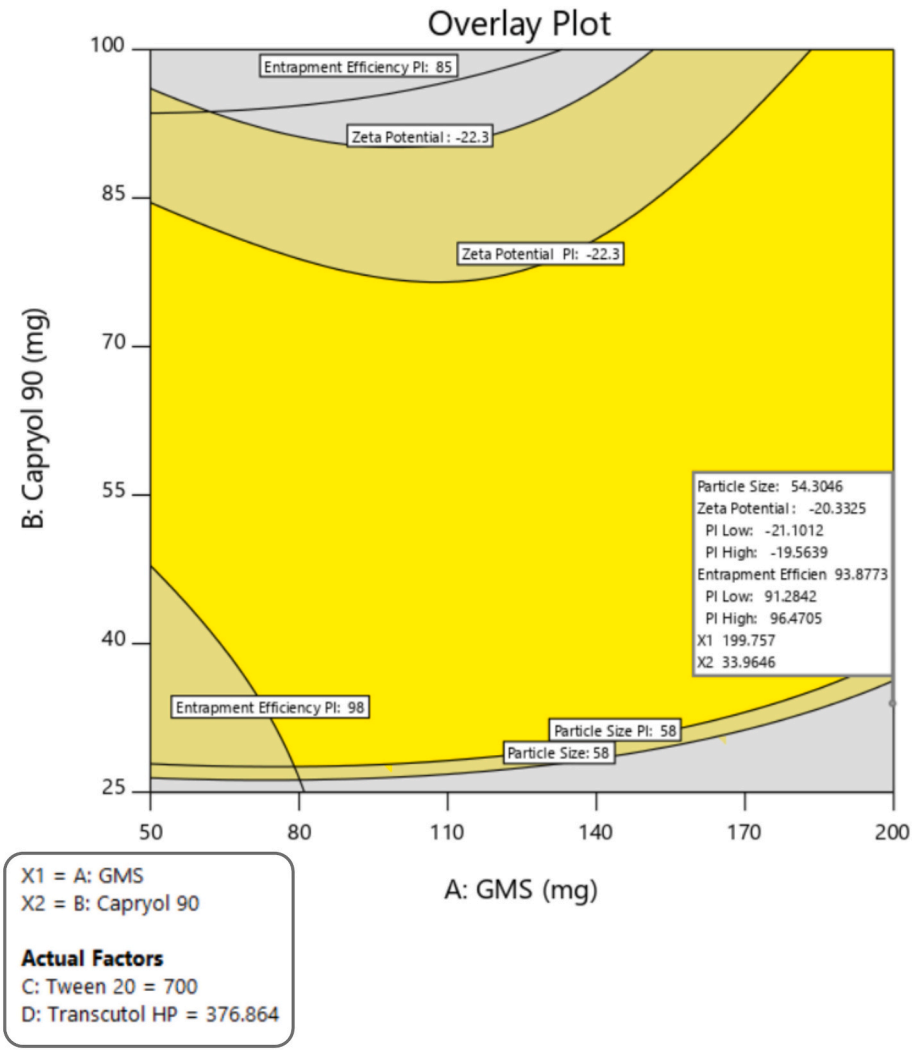

Fig. 8. Overlay plot showing the predicted values and responses for formulation of NLCs.

equations and final mathematical model was determined. The counter plots for various independent factors were plotted by these equations [50].

$$PS = 169.60 - 38.27A + 14.59\,B + 2.38\,C - 5.42\,D - 14.9AB + 19.15\,AC - 12.05AD + 2.59\,BC + 31.12\,BD - 26.44\,CD - 6.47A^2 - 33.22\,B^2 + 46.69C^2 - 7.41D^2 \quad \text{equation (3)}$$

$$ZP = -19.72 - 0.0692A - 0.3667\,B - 0.6233\,C + 0.3158\,D + 0.6550AB - 0.1300AC + 0.9625\,AD - 0.6500BC + 0.2650\,BD - 1.80CD + 0.9100A^2 - 0.5763B^2 - 0.46C^2 + 0.6150\,D^2 \quad \text{equation (4)}$$

$$\%\,EE = 94.80 + 0.5833A - 1.92B - 1.25C - 0.75500D + 2.25AB - 0.2500AD - 2.25\,BC + 2.25BD - 3.25CD + 1.48A^2 - 2.02B^2 + 0.7250C^2 - 3.28D^2 \quad \text{equation (5)}$$

The positive and negative sign of PE indicates the synergistic and antagonistic effects against the responses respectively. The PE indicated that the PS was decreased with increase in factor A and D, where as it is increased with increase in factor B and C. ZP was decreased with increase in factor A, B and C, while it is increased with increase in factor A and decreased with increase of factor B, C and D. The perturbation plots were also plotted to understand the effect of factors on the responses. The straight and flat lines of these plots indicated no impact of factor on responses where as a significant impact was indicated by steep and bent curves [51].

The perturbation plot shown in Fig. 4a, indicated that, factor C was more dominant than other factor A, B and C on PS. Similarly, perturbation plot shown in Fig. 4b, showed that factor B has more dominant effect than other A, C and D factors on ZP. Similarly, perturbation plot shown in Fig. 4c indicated that factor D had more dominant effect on % EE than the other factors A, B and C for CS.

The obtained polynomial equations helped in establishment of 3D response surface plots (3D-RSP), shown in Fig. 5a-f. The 3D-RSP (Fig. 5a) indicated a decrease in PS with increase in factor A and decrease in factor B. Fig. 5b indicated, increase in factor A and C resulted in decreased particle size. Similarly, Fig. 5c indicated that increase in factor A and D resulted in decreased PS. In the same manner Fig. 5d revealed that decrease in factor B and increase of factor C resulted in reduction of the PS. Correspondingly Fig. 5e indicated that decrease in factor B and increase in factor D caused reduction in particle size. Identically, Fig. 5f represented that increase in factor C and D levels caused reduction in PS.

Fig. 6a indicated that increase in factor A and B shifted the ZP towards negative side. Fig. 6b represented increase in factor A and C shifted the negative value of ZP towards higher side. Fig. 6c indicated

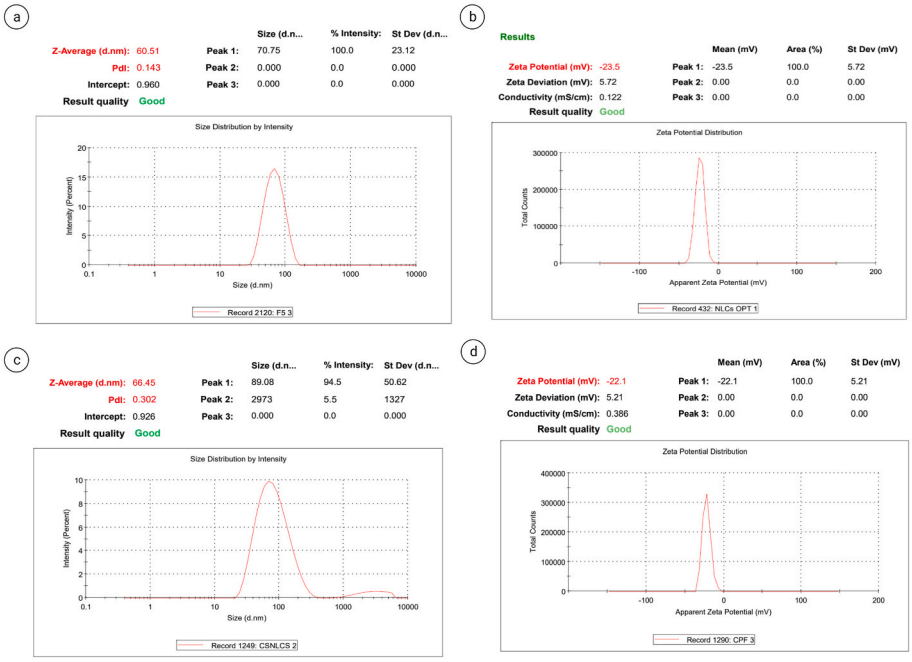

Fig.9. (a–b). PS and ZP of optimized CS-NLCs(c-d) CS-NLCs+PB loaded gel of PS and ZP.

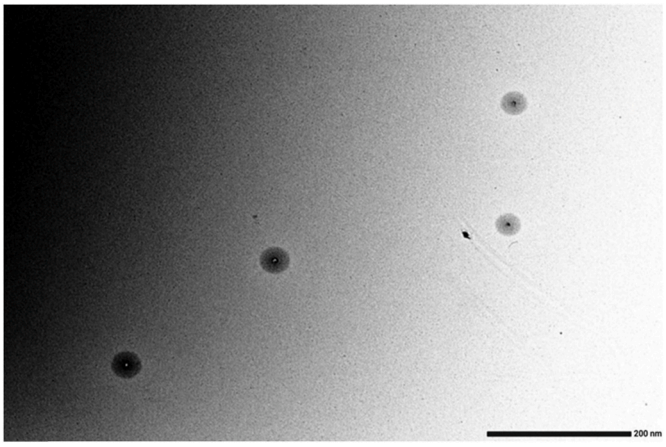

Fig. 10. Morphology of the CS loaded NLCs.

that higher the value of factor A and D more the negative value of ZP. Similarly, Fig. 6d represented as the increase in factor B and C resulted in higher negative sign of ZP. Similarly, Fig. 6e showed that the increase in factor B and D shifted the ZP value towards more negative side. Similarly increase in factor C and decrease in factor D shifted the ZP value towards more negative side (Fig. 6f).

The 3D RSPs for % EE were shown in Fig. 7a-f. In Fig. 7a increased % EE was observed with increase in factor A and B. Similarly increase in factor A and C resulted in increased the % EE (Fig. 7b.). Similarly increase in factor A, D (Fig. 7c.), B, C (Fig.7d), B, D (Fig. 7e) C and D (Fig. 7f) resulted in increased % EE.

3.4. Graphical optimization of CS loaded NLCs

As per the BBD, the optimized values for various parameters, which include solid lipid, liquid lipid, surfactant and co surfactant was found to be 199.99 mg, 33.92 mg, 700 mg and 376.869 mg, respectively shown in Fig. 8.

The BBD design suggested that using above mentioned values, CS loaded NLCs can be formulated having the PS in the range of 50.32–57.98 nm, ZP in the range of −21.09 to −19.55 mV and % EE in the range of 91–96. The reproducibility of the developed NLCs containing CS was confirmed by characterizing them for PS, ZP and % EE. The experiments were performed in triplicate and mean data with SD was recorded. It was indicated that the predicted composition was authenticated. The obtained values of PS, and ZP were found to be 60 ± 2.312 nm (Fig. 9a) and −23.5 ± 5.72 mV (Fig. 9b) respectively. These values were in close agreement with predicted values as p value was found more than 0.05,which is mentioned in Table 6. There was a good correlation between predicted and obtained values and it indicated suitability and reproducibility of DoE. The PDI value of optimized NLCs was 0.143.

3.5. Characterization of CS–PB NLCs

3.5.1. PS

The PS of the CS NLCs and PB loaded gel was found to be 66.45 ± 5.62 nm with a PDI value of 0.302 (Fig. 9c–d). It is pertinent to add that the particle size of NLCs present in the gel did not affect due to gel formation and addition of PB. There are similar studies wherein no significant change in PS has been observed after converting NLCs into gel [50,52]. However, the PDI values of CS-NLCs after adding them into gel along with probiotics got slightly enhanced. Even though the values of PDI was less than 0.4, indicating homogenous dispersion of nanoparticles in the formulation.

3.5.2. ZP

The ZP of CS NLCs was found to be −22.1 ± 5.21 mV (Fig. 9a–d). Like PS, the ZP of NLCs present in the gel did not affect gel formation. It is important to state here that, ideally ±30 mV of ZP is required to stabilize a nanoparticle. However, there are many studies wherein successful development of NLCs have been reported with a ZP of ±15 to ±20 mV [53,54]. This could be because of presence of lipids (GMS, C-90) as well as surfactants (T-20 and T-HP) due to generation of steric as well as electrostatic stabilization to the formulation leading to the generation of permanent repulsive forces between the nanoparticles [52]. The negative ZP of formulation is an indication that the presence of the repulsive forces in between the particles and the dispersion system was more stable. According to the DLVO theory repulsive forces are

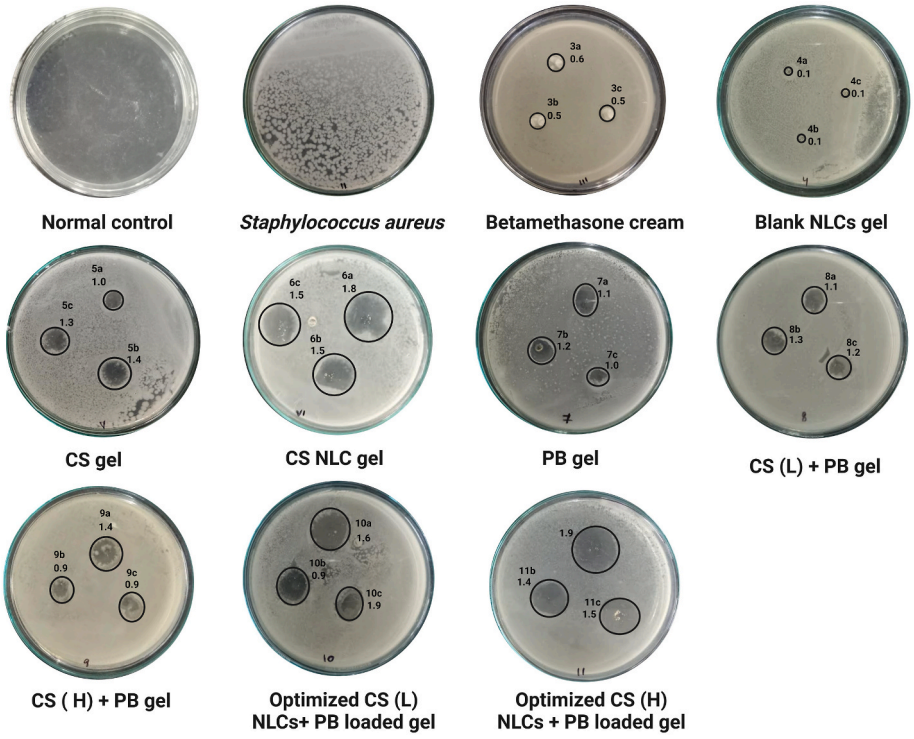

Fig. 11. Zone of inhibition for various treatment groups.

Table 7
Anti-bacterial study of CS and probiotic loaded NLCs.

Group no.	Groups	Treatment	Dosage	No. of petri-plates	Results
I	Normal control	Normal saline (No induction)	Spreaded on the solidified agar media	3	No growth was observed which indicated as the medium was not contaminated and sterilized
Staphylococcus aureus spreaded on the solidified agar petri-plates					
II	Experimental control	*Staphylococcus aureus* (Test organism)	50 billion CFU spreaded on the solidified agar media	3	Round shaped colonies growth was observed, (Staphylococcus aureus)
III	Positive control	Marketed Betamethasone cream	0.1% w/w filled in the 3 bores in each petri-plate	3	No inhibition observed
IV	Treatment I	Blank NLCs gel	Filled in the 3 bores in each petri-plate	3	No inhibition observed
V	Treatment II	CS gel	0.006% w/w of CS gelfilled in the 3 bores in each petri-plate	3	1.23 ± 0.208 cm diameter of zone of inhibition was observed
VI	Treatment III	CS NLCs gel	0.006% w/w of CS NLCs gel filled in the 3 bores in each petri-plate	3	1.33 ± 0.288 cm diameter of zone of inhibition was observed
VII	Treatment IV	PB gel	10 Billions CFU BI filled in the 3 bores in each petri-plate	3	1.10 ± 0.100 cm diameter of zone of inhibition was observed
VIII	Treatment V	CS (L) + PB gel	0.003% w/wof CS + 10 billions CFU BI loaded filled in the 3 bores in each petri-plate	3	1.20 ± 0.100 cm diameter of zone of inhibition was observed
IX	Treatment VI	CS (H) + PB gel	0.003% w/w of CS + 10 billions CFU BI loaded filled in the 3 bores in each petri-plate	3	1.06 ± 0.288 cm diameter of zone of inhibition was observed
X	Treatment VII	Optimized CS NLCs (L) + PB loaded gel	0.0025% w/w of CS + 10 billions CFU BI loaded NLCs filled in the 3 bores in each petri-plate	3	1.46 ± 0.513 cm diameter of zone of inhibition was observed
XI	Treatment VIII	Optimized CS NLCs (H) + PB loaded gel	0.005% w/wof CS + 10 billions CFU BI loaded filled in the 3 bores in each petri-plate	3	1.60 ± 0.264 cm diameter of zone of inhibition was observed

more dominating the Vander walls attractive forces, it forms a more stable formulation [51].

3.5.3. EE and DL

The % EE refers to the amount of drug encapsulated when compared with the total amount of drug added initially. % DL defined as the amount of drug encapsulated when compared with the amount of total lipids added in dispersion [55].

The % EE of the CS- NLCs and PB loaded gel was found to be 97.25 ± 0.15%. This may be due to the proportion of solid lipid to liquid lipid ratio as well as the type of liquid lipid used i.e., C-90. In addition, lower molecular weight (CS: 254.4), higher solubility of drug in lipid might helped to obtain higher % EE. It may also attributed due to the formation of imperfections in the lipid matrix [56].

The % DL of the CS in CS NLCs and PB loaded gel NLCs was found to be 82.3 ± 1.04%. It may be due to the formation of imperfections by the solid lipid and liquid lipid mixture, which offers more space for accommodation of drug [57]. This may also attributed to the higher solubility of CS in lipid matrix [58].

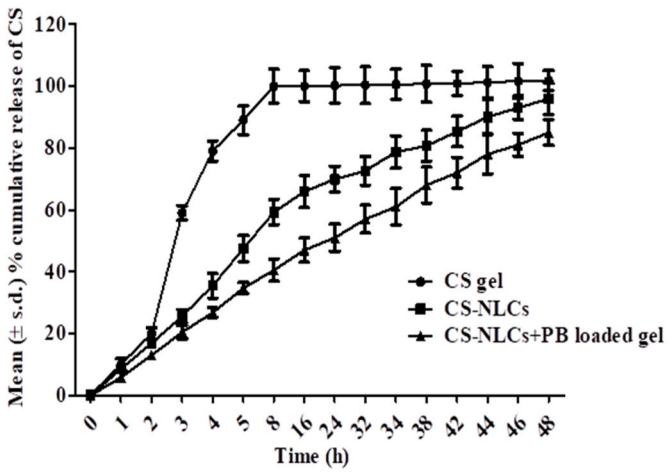

Fig. 12. *In vitro* diffusion study of CS gel, CS-NLCs, CS-NLCs + PB loaded gel.

Table 8
Release kinetics of CS from CS- NLCs + PB loaded gel and CS-NLCs.

Release kinetics	Plot	CS-NLCs PB loaded gel(R^2)	CS-NLCs
Zero order	Time "Vs" % CDR	0.863	0.726
First order	Time "Vs" log % CDR	0.612	0.600
Hixson Crowel	Time "Vs" % Cumulative drug remaining	0.225	0.315
Higuchi	square root of time "Vs" % CDR	0.993	0.981
Korsmeyer-peppas model	Log time "Vs" Log % CDR	0.991	0.992

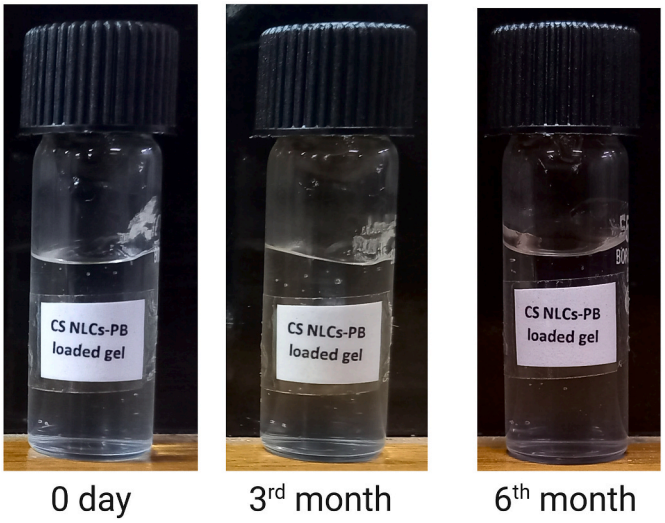

Fig. 13. Images of CS-NLCs PB loaded gel tested on 0 day, 3rd and 6th months.

3.5.4. TEM

The external morphological structure of CS NLCs (Fig. 10) was found to be smooth spherical in shape without aggregation of particles. The tentative particle size of TEM was in the range of 60–72 nm. The particle size obtained from TEM results were slightly less than that of the result that was obtained from DLS for this formulation. However, the difference between results of particle size obtained through TEM and DLS was insignificant ($p > 0.05$) [59,60]. Hence, they were considered similar.

Table 9
Stability studies of CS-NLCs PB loaded gel.

Formulation evaluation Time period	Physical appearance	PS (nm)	ZP (mV)	PDI	EE (%)
At the time of preparation	Transparent	66.45 ± 50.62	−22.1 ± 5.21	0.30	98% ± 0.26
3rd month	Transparent	66.81 ± 98.23	−20.3 ± 7.47	0.21	98% ± 0. 32
6th month	Transparent	73.75 ± 50.07	−19.3 ± 4.65	0.25	96% ± 0. 32

3.5.5. Antibacterial study

The antibacterial study for CS NLCs and PB loaded gel-was performed by the use of *Staphylococcus aureus*. The zone of inhibition (ZOI) (Fig. 11.) for all the treated groups was observed except for group III and IV which include marketed Betamethasone acted as positive control and blank NLCs respectively. The zone of inhibition of CS-NLCs+PB loaded gel was 0.5-fold, 0.2-fold and 0.54-fold higher than PB alone, CS alone and CS-PB combination, respectively. It indicated significantly higher antibacterial activity of CS-NLCs+PB loaded gel (Fig. 11) as that of any other treatment group (Table 7).

3.5.6. In vitro diffusion studies of naive CS gel, CS- NLCs, CS-NLCs + PB loaded gel

The study was aimed to develop CS-NLCs + PB loaded gel in order to get a prolonged release of CS at the site of skin disease like psoriasis with better spreadability of drug on the wound area. Owing to this objective the release study was conducted for naive CS gel, CS-NLCs and CSNLCs + PB loaded gel. It was inferred from the study that in the initial 8 h of the study, 100% of CS got released from the naive CS gel. This indicated its faster release profile. However, the release of CS from CS-NLCs was about 55.24 ± 4.11% and CS from CS-NLCs + PB loaded gel was about 40.47 ± 3.650% in the initial 8 h. This indicated a sustained release profile of CS-NLCs and CS-NLCs + PB loaded gel. The decrease in release of CS from CS-NLCs and CS-NLCs + PB loaded gel as compared to naive CS gel was found to be 1.69 fold and 2.5 folds respectively. This may be due to matrix effect of GMS and CAP-90. The compact structure of the GMS matrix allowing liquid flow, its internal molecular organization, and the size of the network mesh can all affect drug release dissolved in liquid phase, as it hinders free diffusion [61]. Similar types of results were observed in previous studies also [22]. It was also observed that the release of CS from CS-NLCs + PB loaded gel was about 1.13-fold lesser as that of CS-NLCs. This could be due to the presence of poly-saccharides, that present in the PB blend that would have further restricted the release of CS from the CS-NLCs + PB loaded gel. This was attributed due to the intact swollen microparticles of poly-saccharide which hinders the release of CS by holding it within the matrix (Fig. 12) [62].

The release pattern of CS-NLCs + PB loaded gel was investigated through different release kinetic release studies i.e., zero order, first order, Hixson Crowel, Higuchi's and Korsmeyer-Peppas equations (Table 8). The results revealed that release pattern of CS-NLCs + PB loaded gel did not follow first order ($R^2 = 0.612$), zero order ($R^2 = 0.863$) and Hixson crowel ($R^2 = 0.225$) Kinetics. The release pattern was best fitted for Higuchi's for CS-NLCs + PB loaded gel and also CS-NLCs which indicated the sustained release and further it has followed korsmeyer-Peppas kinetics which indicated the release of CS through diffusion process. For further confirmation on release pattern, of CS-NLCs + PB loaded gel and CS-NLCs release study was checked with korsmeyer-peppas equation. It was found that the release exponent 'n' is more than 0.45 which indicated the fickian diffusion type of release from CS-NLCs + PB loaded gel and also CS-NLCs [63]. Moreover, several studies revealed that, the mechanism of drug release followed drug diffusion through the lipid matrix from NLCs [64,65].

3.5.7. Stability studies

The stability studies for the CS-NLCs + PB loaded gel were carried out for a period of 6 months and samples were withdrawn at third month and sixth month. The samples were evaluated for physical appearance, PS, PDI, ZP and % EE. Both samples (3rdand 6th month) were found transparent (Fig. 13) and matched with transparency of freshly prepared formulation. Further no significant changes in PS, ZP and %EE of CS-PB NLCs was observed when compared to freshly prepared formulation (Table 9). Hence the CS-NLCs + PB loaded gel were considered to be stable. The PDI values of the formulation were slightly reduced in 3rd month and 6th month when compared to the PDI value of fresh formulation. Even though the values of PDI was less than 0.4, indicating homogenous dispersion of nanoparticles in the formulation.

4. Conclusion

In present study an attempt has been made to develop the chrysin nano lipid carriers with PB loaded gel by modified hot homogenization followed by sonication technique via Box Behnken Design (BBD). BBD has aided in comprehending the factors and guiding the design process for the formulation of NLCs. The 3D response surface plots, polynomial equations and perturbation plots helped in prediction and validation of the values of selected independent variables for the formulation of optimized CS NLCs with probiotic gel with desired particle size (66.45 nm), zeta potential (−22.1 mV) and % entrapment efficiency (97.25%). The use of optimized GMS and C90 as lipids proved to be effective carrier for developing NLCs as it showed excellent entrapment efficiency. The optimized formulation values were found to be 199.99 mg, 33.92 mg, 700 mg and 376.86 mg of solid lipid, liquid lipid, surfactant and co-surfactant respectively. In addition to that particle size of chrysin nano lipid carriers (CS-NLCs) waswithin the nano meter range. The morphological study of CS-NLCs revealed spherical shape as confirmed by transmission electron microscopy imaging. The release of CS from CS NLCs was found to be 98% in sustained manner. The developed optimized formulation was more stable, which was confirmed by the zeta potential above −15 mV. The results of antibacterial studies revealed highest zone of inhibition as a result of treatment with CS-NLCs + PB loaded gel as compared to naive chrysin gel, naive probiotic gelalone and CS-NLCs, indicating the potential of developed formulation. The positive outcomes of the *in vitro* studies indicate towards its exploration on suitable *in vivo* animal model so that a novel topical formulation for treating dermatological diseases could be brought for clinical application.

CRediT authorship contribution statement

Shaik Rahana Parveen: Methodology, Data Curation and Writing - original draft, Sheetu Wadhwa: Conceptualization, Supervision and Writing - review & editing, Molakpogu Ravindra Babu: Methodology, Review & editing, Sukriti Vishwas: Methodology, Review & editing, Leander Corrie: Methodology, Review & editing, Ankit Awasthi: Methodology, Review & editing, Farhan R. Khan: Methodology, Review & editing, Maha M. Al-Bazi: Methodology, Review & editing, Nahed S. Alharthi: Methodology, Review & editing, Faisal Alotaibi: Methodology, Review & editing, Gaurav Gupta: Methodology, Review & editing, Narendra Kumar Pandey: Methodology, Review & editing, Bimlesh Kumar: Methodology, Review & editing, Popat Kumbhar: Methodology, Review & editing, John Disouza: Methodology, Review & editing, Monica Gulati: Supervision and Writing - review & editing, Jayanthi Neelamraju: Methodology, Review & editing, Resources, Ratna Sudha Madempudi: Methodology, Review & editing, Resources, Kamal Dua: Methodology, Review & editing, Sachin Kumar Singh: Conceptualization, Validation, Supervision and Writing - review & editing.

Declaration of competing interest

The authors declare no conflict of interest.

Data availability

Data will be made availablefo on request.

Acknowledgments

Authors are thankful to Central Instrumentation Facility, Lovely Professional University for providing necessary support in terms of sample analysis using sophisticated instruments such as SEM and HPLC. Authors are also thankful to Unique Biotech, Hyderabad, Telangana, India for providing the gift sample of probiotics as well as guidance. Authors are thankful to Embase database, Elsevier for providing literature support.

References

[1] M. Talebi, M. Talebi, T. Farkhondeh, D.M. Kopustinskiene, J. Simal-Gandara, J. Bernatoniene, S. Samarghandian, An updated review on the versatile role of chrysin in neurological diseases: chemistry, pharmacology, and drug delivery approaches, Biomed. Pharmacother. 141 (2021), https://doi.org/10.1016/J.BIOPHA.2021.111906.

[2] S. Naz, M. Imran, A. Rauf, I.E. Orhan, M.A. Shariati, Iahtisham-Ul-Haq, IqraYasmin, M. Shahbaz, T.B. Qaisrani, Z.A. Shah, S. Plygun, M. Heydari, Chrysin: pharmacological and therapeutic properties, Life Sci. 235 (2019), https://doi.org/10.1016/J.LFS.2019.116797.

[3] R. Mani, V. Natesan, Chrysin: sources, beneficial pharmacological activities, and molecular mechanism of action, Phytochemistry 145 (2018) 187–196, https://doi.org/10.1016/J.PHYTOCHEM.2017.09.016.

[4] H.J. Li, N.L. Wu, C.M. Pu, C.Y. Hsiao, D.C. Chang, C.F. Hung, Chrysin alleviates imiquimod-induced psoriasis-like skin inflammation and reduces the release of CCL20 and antimicrobial peptides, Sci. Rep. 10 (2020), https://doi.org/10.1038/S41598-020-60050-1.

[5] A. Siddiqui, Badruddeen, J. Akhtar, M.S S. Uddin, M.I. Khan, M. Khalid, M. Ahmad, A naturally occurring flavone (chrysin): chemistry, occurrence, pharmacokinetic, toxicity, molecular targets and medicinal properties, J. Biol. Act. Prod. from Nat. 8 (2018) 208–227, https://doi.org/10.1080/22311866.2018.1498750.

[6] S. Jindal, R. Awasthi, D. Singhare, G.T. Kulkarni, Topical delivery of Tacrolimus using liposome containing gel: an emerging and synergistic approach in management of psoriasis, Med. Hypotheses 142 (2020), https://doi.org/10.1016/J.MEHY.2020.109838.

[7] S.S. Pandey, M.A. Patel, D.T. Desai, H.P. Patel, A.R. Gupta, S.V. Joshi, D.O. Shah, F. A. Maulvi, Bioavailability enhancement of repaglinide from transdermally applied nanostructured lipid carrier gel: optimization, in vitro and in vivo studies, J. Drug Deliv. Sci. Technol. 57 (2020), 101731, https://doi.org/10.1016/j.jddst.2020.101731.

[8] U.U. Mohd Nordin, N. Ahmad, N. Salim, N.S. Mohd Yusof, Lipid-based nanoparticles for psoriasis treatment: a review on conventional treatments, recent works, and future prospects, RSC Adv. 11 (2021) 29080–29101, https://doi.org/10.1039/D1RA06087B.

[9] J.A. Carroll, K. C, J.A. Hobden, S. Miller, S.A. Morse, T.A. Mietzner, B. Detrick, T. G. Mitchell, J.H. McKerrow, Sakanari, Normal Human Microbiota, McGraw-Hill Education, New York, NY, 2019.

[10] F. Argentina, R. Rusmawardiana, G. Garfendo, Skin microbiota, Maj. Kedokt. Sriwij. 52 (2020) 233–238.

[11] D.K. Hsu, M.A. Fung, H.-L. Chen, Role of skin and gut microbiota in the pathogenesis of psoriasis, an inflammatory skin disease, Med. Microecol. 4 (2020), 100016, https://doi.org/10.1016/j.medmic.2020.100016.

[12] L. Chen, J. Li, W. Zhu, Y. Kuang, T. Liu, W. Zhang, X. Chen, C. Peng, Skin and gut microbiome in psoriasis: gaining insight into the pathophysiology of it and finding novel therapeutic strategies, Front. Microbiol. 11 (2020), https://doi.org/10.3389/FMICB.2020.589726.

[13] M. Gupta, J.M. Weinberg, P.S. Yamauchi, A. Patil, S. Grabbe, M. Goldust, Psoriasis: embarking a dynamic shift in the skin microbiota, J. Cosmet. Dermatol. 21 (2022) 1402–1406, https://doi.org/10.1111/JOCD.14273.

[14] Y.H. Chen, C.S. Wu, Y.H. Chao, C.C. Lin, H.Y. Tsai, Y.R. Li, Y.Z. Chen, W.H. Tsai, Y. K. Chen, Lactobacillus pentosus GMNL-77 inhibits skin lesions in imiquimod-induced psoriasis-like mice, J. Food Drug Anal. 25 (2017) 559–566, https://doi.org/10.1016/J.JFDA.2016.06.003.

[15] I.A. Rather, V.K. Bajpai, Y.S. Huh, Y.K. Han, E.A. Bhat, J. Lim, W.K. Paek, Y. H. Park, Probiotic Lactobacillus sakei proBio-65 extract ameliorates the severity of imiquimod induced psoriasis-like skin inflammation in a mouse model, Front. Microbiol. 9 (2018), https://doi.org/10.3389/FMICB.2018.01021.

[16] D. Groeger, L. O'Mahony, E.F. Murphy, J.F. Bourke, T.G. Dinan, B. Kiely, F. Shanahan, E.M.M. Quigley, Bifidobacterium infantis 35624 modulates host inflammatory processes beyond the gut, Gut Microb. 4 (2013) 325–339, https://doi.org/10.4161/GMIC.25487.

[17] S.K. Morris, Skin Microbiome Colonizer Formulations and Methods for Use, 2020.
[18] B. Subramaniam, Z.H. Siddik, N.H. Nagoor, Optimization of nanostructured lipid carriers: understanding the types, designs, and parameters in the process of formulations, J. Nanoparticle Res. 22 (2020) 1–29.
[19] A. Awasthi, B. Kumar, M. Gulati, S. Vishwas, L. Corrie, J. Kaur, R. Khursheed, R. A. Muhammed, D. Kala, O. Porwal, M.R. Babu, M.V.N.L. Chaitanya, A. Kumar, N. K. Pandey, H. Dureja, D.K. Chellappan, N.K. Jha, G. Gupta, P. Prasher, D. Kumar, K. Dua, S.K. Singh, Novel nanostructured lipid carriers Co-loaded with mesalamine and curcumin: formulation, optimization and in vitro evaluation, Pharm. Res. (N. Y.) 39 (2022), https://doi.org/10.1007/S11095-022-03401-Z.
[20] S. Das, W.K. Ng, P. Kanaujia, S. Kim, R.B.H. Tan, Formulation design, preparation and physicochemical characterizations of solid lipid nanoparticles containing a hydrophobic drug: effects of process variables, Colloids Surf. B Biointerfaces 88 (2011) 483–489, https://doi.org/10.1016/j.colsurfb.2011.07.036.
[21] B. Shah, D. Khunt, H. Bhatt, M. Misra, H. Padh, Application of quality by design approach for intranasal delivery of rivastigmine loaded solid lipid nanoparticles: effect on formulation and characterization parameters, Eur. J. Pharm. Sci. Off. J. Eur. Fed. Pharm. Sci. 78 (2015) 54–66, https://doi.org/10.1016/j.ejps.2015.07.002.
[22] V. Harish, D. Tewari, S. Mohd, P. Govindaiah, M.R. Babu, R. Kumar, M. Gulati, K. Gowthamarajan, S.V. Madhunapantula, D.K. Chellappan, G. Gupta, K. Dua, S. Dallavalasa, S.K. Singh, Quality by design based formulation of xanthohumol loaded solid lipid nanoparticles with improved bioavailability and anticancer effect against PC-3 cells, Pharmaceutics 14 (2022) 2403, https://doi.org/10.3390/PHARMACEUTICS14112403.
[23] B. Gaba, M. Fazil, S. Khan, A. Ali, S. Baboota, J. Ali, Nanostructured lipid carrier system for topical delivery of terbinafine hydrochloride, Bull. Fac. Pharm. Cairo Univ. 53 (2015) 147–159.
[24] M.H. Kim, K.T. Kim, S.Y. Sohn, J.Y. Lee, C.H. Lee, H. Yang, B.K. Lee, K.W. Lee, D. D. Kim, Formulation and evaluation of nanostructured lipid carriers (NLCs) of 20 (S)-Protopanaxadiol (PPD) by box-behnken design, Int. J. Nanomed. 14 (2019) 8509–8520, https://doi.org/10.2147/IJN.S215835.
[25] K.S. Kim, J.S. Shin, Y. Park, S. Lee, Y.B. Kim, B.-K. Kim, High-performance liquid chromatographic analysis of chrysin derivatives on a Nova-Pak C18 column, Arch Pharm. Res. (Seoul) 25 (2002) 613–616, https://doi.org/10.1007/BF02976930.
[26] M.D. Joshi, R.H. Prabhu, V.B. Patravale, Fabrication of nanostructured lipid carriers (NLC)-Based gels from microemulsion template for delivery through skin, Methods Mol. Biol. (2000) 279–292, https://doi.org/10.1007/978-1-4939-9516-5_19, 2019.
[27] R. Rani, S. Dahiya, D. Dhingra, N. Dilbaghi, K.H. Kim, S. Kumar, Improvement of antihyperglycemic activity of nano-thymoquinone in rat model of type-2 diabetes, Chem. Biol. Interact. 295 (2018) 119–132, https://doi.org/10.1016/J.CBI.2018.02.006.
[28] A.L. Ajiboye, U. Nandi, M. Galli, V. Trivedi, Olanzapine loaded nanostructured lipid carriers via high shear homogenization and ultrasonication, Sci. Pharm. 89 (2021) 25.
[29] N. Mauro, C. Fiorica, P. Varvarà, G. Di Prima, G. Giammona, A facile way to build up branched high functional polyaminoacids with tunable physicochemical and biological properties, Eur. Polym. J. 77 (2016) 124–138.
[30] G. Angellotti, A. Presentato, D. Murgia, G. Di Prima, F. D'Agostino, A.G. Scarpaci, M.C. D'Oca, R. Alduina, G. Campisi, V. De Caro, Lipid nanocarriers-loaded nanocomposite as a suitable platform to release antibacterial and antioxidant agents for immediate dental implant placement restorative treatment, Pharmaceutics 13 (2021) 2072.
[31] I. Chauhan, M. Yasir, M. Verma, A.P. Singh, Nanostructured lipid carriers: a groundbreaking approach for transdermal drug delivery, Adv. Pharmaceut. Bull. 10 (2020) 150–165, https://doi.org/10.34172/APB.2020.021.
[32] K.H. Bang, Y.G. Na, H.W. Huh, S.J. Hwang, M.S. Kim, M. Kim, H.K. Lee, C.W. Cho, The delivery strategy of paclitaxel nanostructured lipid carrier coated with platelet membrane, Cancers 11 (2019), https://doi.org/10.3390/CANCERS11060807.
[33] I. Jazuli, B. Nabi Annu, T. moolakkadath, T. Alam, S. Baboota, J. Ali, Optimization of nanostructured lipid carriers of lurasidone hydrochloride using box-behnken design for brain targeting: in vitro and in vivo studies, J. Pharm. Sci. 108 (2019) 3082–3090, https://doi.org/10.1016/J.XPHS.2019.05.001.
[34] N. Üstündağ-Okur, E.H. Gökçe, D.I. Bozbiyik, S. Eğrilmez, Ö. Özer, G. Ertan, Preparation and in vitro-in vivo evaluation of ofloxacin loaded ophthalmic nano structured lipid carriers modified with chitosan oligosaccharide lactate for the treatment of bacterial keratitis, Eur. J. Pharmaceut. Sci. 63 (2014) 204–215, https://doi.org/10.1016/J.EJPS.2014.07.013.
[35] A.K. Ramanunny, S. Wadhwa, S. Kumar Singh, B. Kumar, M. Gulati, A. Kumar, S. Almawash, A. Al Saqr, K. Gowthamarajan, K. Dua, H. Singh, S. Vishwas, R. Khursheed, S. Rahana Parveen, A. Venkatesan, K.R. Paudel, P.M. Hansbro, D. Kumar Chellappan, Topical non-aqueous nanoemulsion of Alpinia galanga extract for effective treatment in psoriasis: in vitro and in vivo evaluation, Int. J. Pharm. 624 (2022), https://doi.org/10.1016/J.IJPHARM.2022.121882.
[36] L. Corrie, J. Kaur, A. Awasthi, S. Vishwas, M. Gulati, S. Saini, B. Kumar, N. K. Pandey, G. Gupta, H. Dureja, D.K. Chellapan, K. Dua, D. Tewari, S.K. Singh, Multivariate data analysis and central composite design-oriented optimization of solid carriers for formulation of curcumin-loaded solid SNEDDS: dissolution and bioavailability assessment, Pharmaceutics 14 (2022) 2395, https://doi.org/10.3390/PHARMACEUTICS14112395.
[37] D. Tamarkin, H. Shifrin, R. Keynan, E. Ziv, T. Berman, D. Schuz, E. Gazal, Oil Foamable Carriers and Formulations, 2022.
[38] P.A. Ittadwar, P.K. Puranik, Analytical method development, characterization, evaluation of in-vitro antioxidant and anticancer activity of flavone chrysin in HeLa cells, Int. J. Pharmaceut. Sci. Drug Res. 13 (2021), https://doi.org/10.25004/IJPSDR.2021.130502.
[39] T. Sharma, O.P. Katare, A. Jain, S. Jain, D. Chaudhari, B. Borges, B. Singh, QbD-steered development of biotin-conjugated nanostructured lipid carriers for oral delivery of chrysin: role of surface modification for improving biopharmaceutical performance, Colloids Surf. B Biointerfaces 197 (2021), https://doi.org/10.1016/J.COLSURFB.2020.111429.
[40] M. Sabzichi, J. Mohammadian, R. Bazzaz, M.B. Pirouzpanah, M. Shaaker, H. Hamishehkar, H. Chavoshi, R. Salehi, N. Samadi, Chrysin loaded nanostructured lipid carriers (NLCs) triggers apoptosis in MCF-7 cancer cells by inhibiting the Nrf2 pathway, Process Biochem. 60 (2017) 84–91.
[41] S.M. Sindhoor, M. Koland, Topical delivery of apremilast loaded nanostructured lipid carrier based hydrogel for psoriasis therapy, J. Pharm. Res. Int. 33 (2021) 7–20.
[42] P.M. Pimpalshende, R.N. Gupta, Formulation and in-vitro drug released mechanism of CNS acting venlafaxine nanostructured lipid carrier for major depressive disorder, Indian J Pharm Edu Res 52 (2018) 230–240.
[43] M. Apostolou, S. Assi, A.A. Fatokun, I. Khan, The effects of solid and liquid lipids on the physicochemical properties of nanostructured lipid carriers, J. Pharm. Sci. 110 (2021) 2859–2872, https://doi.org/10.1016/J.XPHS.2021.04.012.
[44] Y. Gu, X. Tang, M. Yang, D. Yang, J. Liu, Transdermal drug delivery of triptolide-loaded nanostructured lipid carriers: preparation, pharmacokinetic, and evaluation for rheumatoid arthritis, Int. J. Pharm. 554 (2019) 235–244, https://doi.org/10.1016/J.IJPHARM.2018.11.024.
[45] F.S. Abdel-Salam, A.A. Mahmoud, H.O. Ammar, S.A. Elkheshen, Nanostructured lipid carriers as semisolid topical delivery formulations for diflucortolone valerate, J. Liposome Res. 27 (2017) 41–55, https://doi.org/10.3109/08982104.2016.1149866.
[46] V.M. Ghate, A.K. Kodoth, A. Shah, B. Vishalakshi, S.A. Lewis, Colloidal nanostructured lipid carriers of pentoxifylline produced by microwave irradiation ameliorates imiquimod-induced psoriasis in mice, Colloids Surf. B Biointerfaces 181 (2019) 389–399, https://doi.org/10.1016/J.COLSURFB.2019.05.074.
[47] D.W. Osborne, J. Musakhanian, Skin penetration and permeation properties of transcutol®-neat or diluted mixtures, AAPS PharmSciTech 19 (2018) 3512–3533, https://doi.org/10.1208/S12249-018-1196-8.
[48] L. Corrie, M. Gulati, A. Awasthi, S. Vishwas, J. Kaur, R. Khursheed, R. Kumar, A. Kumar, M. Imran, D.K. Chellappan, Polysaccharide, fecal microbiota, and curcumin-based novel oral colon-targeted solid self-nanoemulsifying delivery system: formulation, characterization, and in-vitro anticancer evaluation, Mater. Today Chem. 26 (2022), 101165.
[49] M. Pradhan, A. Alexander, M.R. Singh, D. Singh, S. Saraf, S. Saraf, K. Yadav, Statistically optimized calcipotriol fused nanostructured lipid carriers for effectual topical treatment of psoriasis, J. Drug Deliv. Sci. Technol. 61 (2021), 102168.
[50] V.K. Rapalli, S. Sharma, A. Roy, G. Singhvi, Design and dermatokinetic evaluation of Apremilast loaded nanostructured lipid carriers embedded gel for topical delivery: a potential approach for improved permeation and prolong skin deposition, Colloids Surf. B Biointerfaces 206 (2021), https://doi.org/10.1016/J.COLSURFB.2021.111945.
[51] S. Rawal, B. Patel, M.M. Patel, Fabrication, optimisation and in vitro evaluation of docetaxel and curcumin Co-loaded nanostructured lipid carriers for improved antitumor activity against non-small cell lung carcinoma, J. Microencapsul. 37 (2020) 543–556, https://doi.org/10.1080/02652048.2020.1823498.
[52] E. Ghazy, A.A. Abdulrasool, J.J. Al-Tamimi, N. Ayash, Nebivolol hydrochloride loaded nanostructured lipid carriers as transdermal delivery system:-part 2:-hydrogel preparation, evaluation and permeation study, tofiq j. Med. Sci. 3 (2016) 1–16.
[53] S.K. Singh, K.K. Srinivasan, K. Gowthamarajan, D.S. Singare, D. Prakash, N. B. Gaikwad, Investigation of preparation parameters of nanosuspension by top-down media milling to improve the dissolution of poorly water-soluble glyburide, Eur. J. Pharm. Biopharm. 78 (2011) 441–446, https://doi.org/10.1016/J.EJPB.2011.03.014.
[54] D.S. Singare, S. Marella, K. Gowthamrajan, G.T. Kulkarni, R. Vooturi, P.S. Rao, Optimization of formulation and process variable of nanosuspension: an industrial perspective, Int. J. Pharm. 402 (2010) 213–220.
[55] V. Savić, T. Ilić, I. Nikolić, B. Marković, B. Čalija, N. Cekić, S. Savić, Tacrolimus-loaded lecithin-based nanostructured lipid carrier and nanoemulsion with propylene glycol monocaprylate as a liquid lipid: formulation characterization and assessment of dermal delivery compared to referent ointment, Int. J. Pharm. 569 (2019), https://doi.org/10.1016/J.IJPHARM.2019.118624.
[56] I.T. Mendes, A.L.M. Ruela, F.C. Carvalho, J.T.J. Freitas, R. Bonfilio, G.R. Pereira, Development and characterization of nanostructured lipid carrier-based gels for the transdermal delivery of donepezil, Colloids Surf. B Biointerfaces 177 (2019) 274–281, https://doi.org/10.1016/J.COLSURFB.2019.02.007.
[57] L. Sahoo, Nanostructured lipid carrier (NLC)—a promising drug delivery for transdermal application, J. Pharmaceut. Sci. Res. 12 (2020) 475–487.
[58] V.C. Gurumukhi, S.B. Bari, Development of ritonavir-loaded nanostructured lipid carriers employing quality by design (QbD) as a tool: characterizations, permeability, and bioavailability studies, Drug Deliv. Transl. Res. 12 (2022) 1753–1773, https://doi.org/10.1007/S13346-021-01083-5.
[59] K. Nayak, S.S. Katiyar, V. Kushwah, S. Jain, Coenzyme Q10 and retinaldehyde co-loaded nanostructured lipid carriers for efficacy evaluation in wrinkles, J. Drug Target. 26 (2018) 333–344, https://doi.org/10.1080/1061186X.2017.1379527.
[60] M.A. Al-Sarraf, A.A. Hussein, Z.A. Al-Sarraf, Comparison between conventional gel and nanostructured lipid carrier gel of zaltoprofen: preparation and in-vitro/ex-vivo evaluation, Technology 11 (2021) 988–995.

[61] R. Hüttenrauch, S. Fricke, Dependence of the release of active principles from ointment bases upon the degree of order of the solid phase, Pharmazie 34 (1979) 437–438.
[62] I. El-Gibaly, Oral delayed-release system based on Zn-pectinate gel (ZPG) microparticles as an alternative carrier to calcium pectinate beads for colonic drug delivery, Int. J. Pharm. 232 (2002) 199–211, https://doi.org/10.1016/S0378-5173(01)00903-6.
[63] S. Dash, P.N. Murthy, L. Nath, P. Chowdhury, Kinetic modeling on drug release from controlled drug delivery systems, Acta Pol. Pharm. 67 (2010) 217–223.
[64] S. Jana, S. Manna, A.K. Nayak, K.K. Sen, S.K. Basu, Carbopol gel containing chitosan-egg albumin nanoparticles for transdermal aceclofenac delivery, Colloids Surf. B Biointerfaces 114 (2014) 36–44.
[65] N.K. Garg, N. Tandel, S.K. Bhadada, R.K. Tyagi, Nanostructured lipid carrier–mediated transdermal delivery of aceclofenac hydrogel present an effective therapeutic approach for inflammatory diseases, Front. Pharmacol. 12 (2021).